4. PRODUCTION AND PROPERTIES OF RADIATIONS

i.e. there is a simple trade off between beam dimension and divergence.

The second type of capillary optic is a monolithic configuration. The individual capillaries in monolithic optics are tapered and fused together, so that no external frame assembly is necessary (Chen-Mayer *et al.*, 1996). Unlike the multifibre devices, the inner diameters of the channels that make up the monolithic optics vary along the length of the component, resulting in a smaller more compact design.

Further applications of capillary optics include small-angle scattering (Mildner, 1994) and lenses for high-spatial-resolution area detection.

4.4.2.5. *Filters*

Neutron filters are used to remove unwanted radiation from the beam while maintaining as high a transmission as possible for the neutrons of the required energy. Two major applications can be identified: removal of fast neutrons and γ-rays from the primary beam and reduction of higher-order contributions (λ/n) in the secondary beam reflected from crystal monochromators. In this section, we deal with non-polarizing filters, *i.e.* those whose transmission and removal cross sections are independent of the neutron spin. Polarizing filters are discussed in the section concerning polarizers.

Filters rely on a strong variation of the neutron cross section with energy, usually either the wavelength-dependent scattering cross section of polycrystals or a resonant absorption cross section. Following Freund (1983), the total cross section determining the attenuation of neutrons by a crystalline solid can be written as a sum of three terms,

$$\sigma = \sigma_{\text{abs}} + \sigma_{\text{tds}} + \sigma_{\text{Bragg}}. \qquad (4.4.2.7)$$

Here, σ_{abs} is the true absorption cross section, which, at low energy, away from resonances, is proportional to $E^{-1/2}$. The temperature-dependent thermal diffuse cross section, σ_{tds}, describing the attenuation due to inelastic processes, can be split into two parts depending on the neutron energy. At low energy, $E \ll k_b \Theta_D$, where k_b is Boltzmann's constant and Θ_D is the characteristic Debye temperature, single-phonon processes dominate, giving rise to a cross section, σ_{sph}, which is also proportional to $E^{-1/2}$. The single-phonon cross section is proportional to $T^{7/2}$ at low temperatures and to T at higher temperatures. At higher energies, $E \geq k_b \Theta_D$, multiphonon and multiple-scattering processes come into play, leading to a cross section, σ_{mph}, that increases with energy and temperature. The third contribution, σ_{Bragg}, arises due to Bragg scattering in single- or polycrystalline material. At low energies, below the Bragg cut-off ($\lambda > 2d_{\text{max}}$), σ_{Bragg} is zero. In polycrystalline materials, the cross section rises steeply above the Bragg cut-off and oscillates with increasing energy as more reflections come into play. At still higher energies, σ_{Bragg} decreases to zero.

In single-crystalline material above the Bragg cut-off, σ_{Bragg} is characterized by a discrete spectrum of peaks whose heights and widths depend on the beam collimation, energy resolution, and the perfection and orientation of the crystal. Hence a mono-crystalline filter has to be tuned by careful orientation.

The resulting attenuation cross section for beryllium is shown in Fig. 4.4.2.7. Cooled polycrystalline beryllium is frequently used as a filter for neutrons with energies less than 5 meV, since there is an increase of nearly two orders of magnitude in the attenuation cross section for higher energies. BeO, with a Bragg cut-off at approximately 4 meV, is also commonly used.

Pyrolytic graphite, being a layered material with good crystalline properties along the *c* direction but random orientation perpendicular to it, lies somewhere between a polycrystal and a single crystal as far as its attenuation cross section is concerned. The energy-dependent cross section for a neutron beam incident along the *c* axis of a pyrolytic graphite filter is shown in Fig. 4.4.2.8, where the attenuation peaks due to the 00ξ reflections can be seen. Pyrolytic graphite serves as an efficient second- or third-order filter (Shapiro & Chesser, 1972) and can be 'tuned' by slight misorientation away from the *c* axis.

Further examples of typical filter materials (*e.g.* silicon, lead, bismuth, sapphire) can be found in the paper by Freund (1983).

Resonant absorption filters show a large increase in their attenuation cross sections at the resonant energy and are therefore used as selective filters for that energy. A list of typical filter materials and their resonance energies is given in Table 4.4.2.3.

4.4.2.6. *Polarizers*

Methods used to polarize a neutron beam are many and varied, and the choice of the best technique depends on the instrument and the experiment to be performed. The main parameter that has to be considered when describing the effectiveness of a given polarizer is the polarizing efficiency, defined as

$$P = (N_+ - N_-)/(N_+ + N_-), \qquad (4.4.2.8)$$

where N_+ and N_- are the numbers of neutrons with spin parallel ($+$) or antiparallel ($-$) to the guide field in the outgoing beam. The second important factor, the transmission of the wanted spin state, depends on various factors, such as acceptance angles, reflection, and absorption.

4.4.2.6.1. *Single-crystal polarizers*

The principle by which ferromagnetic single crystals are used to polarize and monochromate a neutron beam simultaneously is shown in Fig. 4.4.2.9. A field **B**, applied perpendicular to the scattering vector κ, saturates the atomic moments $\mathbf{M}_\nu$ along the field direction. The cross section for Bragg reflection in this geometry is

$$(\,\mathrm{d}\sigma/\,\mathrm{d}\Omega) = F_N(\kappa)^2 + 2F_N(\kappa)F_M(\kappa)(\mathbf{P}\cdot\mathbf{\mu}) + F_M(\kappa)^2, \quad (4.4.2.9)$$
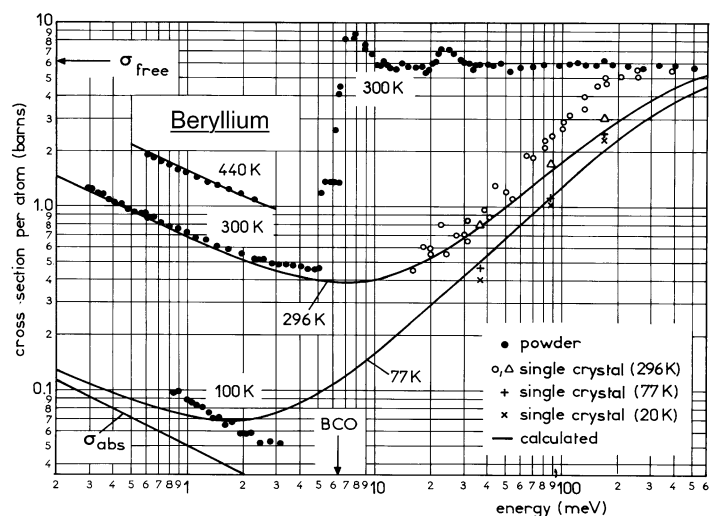

Fig. 4.4.2.7. Total cross section for beryllium in the energy range where it can be used as a filter for neutrons with energy below 5 meV (Freund, 1983).

438